Characterization of Coarse Particles Formed by Laser Ablation of MALDI Matrixes

Shelley N. Jackson, Sushama Mishra, and Kermit K. Murray*
Department of Chemistry, Louisiana State University, Baton Rouge, Louisiana 70803
Received: May 8, 2003; In Final Form: July 22, 2003

The quantity and size distribution of micrometer-sized particles ejected from thin crystalline films of organic molecules was measured with light scattering particle sizing. Four compounds that are commonly used as matrix materials in matrix-assisted laser desorption ionization (MALDI) were studied: 2,5-dihydroxybenzoic acid (DHB), sinapic acid, 4-nitroaniline, and 2-(4-hydroxyphenylazo)benzoic acid (HABA). Thin films of these matrixes were irradiated at atmospheric pressure with a 4 ns pulsed 337 nm nitrogen laser. Particulate resulting from the ablation was sampled directly into a particle sizing instrument. The mean aerodynamic diameter of the coarse particles formed at a laser fluence of 500 J/m^2 was approximately 700 nm for all matrixes. This value does not include particles below 500 nm, which are not accurately measured by the particle sizing instrument. The threshold for detection of particles from the DHB matrix was found to be 300 J/m^2 and it was estimated that an average of 1000 particles in the micrometer size range are ejected per laser shot. The fluence threshold and quantity of material ablated are similar to that observed for MALDI ion formation, suggesting that the role of large particle formation in this process is significant.

Introduction

Although studies of the mechanisms of matrix-assisted laser desorption ionization (MALDI) have lagged its application, there has been a renewed interest in fundamental studies aimed at understanding the processes involved in material desorption, ablation, and ion formation.[1−10] As a result of this heightened interest, an energetic discussion has emerged surrounding the role of clusters in the process of MALDI ion formation. Most models of MALDI ionization have treated the processes of desorption or ablation of material separately from the ionization of the analyte.[1−4,11] In this interpretation, primary matrix ionization occurs in the first few nanoseconds after the laser pulse, followed by secondary ionization of the analyte by collisional transfer of protons, cations, or electrons in the expanding plume of material. A competing cluster ionization mechanism has been proposed in which the desorption and ionization events are considered together.[5−7] According to this mechanism, charged analyte molecules are formed through charge separation and photoionization in ejected matrix clusters. Evaporation of neutral matrix molecules from the clusters and charge reduction by electron capture results in singly charged analyte molecules.

Recent molecular dynamics (MD) simulations of MALDI desorption and ablation support the idea that clusters and small particles are formed under conditions similar to those in MALDI.[8,9,12] In the MD calculations, the matrix molecule is represented by a "breathing sphere" with a single vibrational mode representing the internal energy of the matrix molecule. Molecular excitation is determined from the matrix absorption coefficient at the laser wavelength and vibrational energy is added to the molecules during the time of the simulated laser pulse. These simulations show a distinct transition from thermal desorption of single molecules at low fluences to ablation of clusters and possibly even small particles at higher fluences. Computational requirements have limited these simulations to 150 ps laser pulses, 100 nm ablation depths, and subnanosecond time scales, yet the observation of cluster emission in these studies has led to an increased interest in understanding the role of bulk material ejection in laser desorption ionization.

Despite the potential role of clusters in MALDI ionization, there is little direct experimental evidence of their presence. A number of recent studies have been aimed at identifying the role of clusters in an indirect fashion. For example, the high ratio of axial to radial ion velocity has been taken as evidence for the ejection of clusters in the MALDI plume.[6] Experiments using pH indicator dyes incorporated into matrix crystals suggest that analyte molecules can be incorporated into matrix crystals as multiply protonated "precharged" species that are necessary precursors in cluster ionization processes.[13] Recent studies of ion flight time variation with extraction delay time have been interpreted as evidence for ion formation as a result of decomposition of gas-phase precursor clusters.[14,15] Postionization studies of laser desorbed chrysene have been taken as an indication that laser-desorbed clusters remain intact after having traveled at least 50 μm from the target surface.[16]

A more direct analysis of the physical processes of laser desorption can be accomplished with plume imaging, using laser-induced fluorescence[17−20] or absorption spectroscopy.[20,21] These studies confirm the existence of a forward-peaked ejection of material from the MALDI target.

The measurement of particle size distribution from laser-ablated material has been employed for a number of applications such as laser-ablation sampling for inductively coupled plasma mass spectrometry (ICP-MS),[22,23] material processing,[24] and nanoparticle formation.[25−27] There has been one previous study of particulate ejection from MALDI matrixes.[28] Atomic force microscopy was used to analyze particles ablated from a thin film of 2,5-dihydroxybenzoic acid matrix and poly(ethylene glycol) analyte. The ratio of molecular to particulate ejection was found to be strongly dependent on the laser fluence.

In this article, we report on the measurement of size distributions of coarse particles (>500 nm) obtained after 337 nm UV laser ablation of MALDI matrix thin films at atmospheric pressure. A stainless steel MALDI sample target with a

* Address correspondence to this author. E-mail: kkmurray@lsu.edu. Phone: 225-578-3417. Fax: 225-578-3458.

10.1021/jp030600v CCC: $25.00
Published on Web 11/01/2003

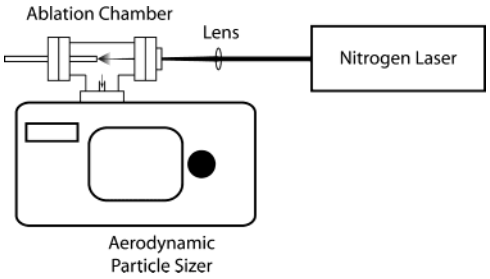

Figure 1. Schematic diagram of the experimental system for laser ablation particle size measurements.

dried-droplet sample preparation was placed in an ablation chamber above the inlet of a light-scattering particle size measuring instrument. After irradiation of the thin film, ablated particulate was sampled by the particle sizer and the particle count and size distribution were recorded. Particle size measurements were made for 2,5-dihydroxybenzoic acid, sinapic acid (*trans*-3,5-dimethoxy-4-hydroxycinnamic acid), 4-nitroaniline, and 2-(4-hydroxyphenylazo)benzoic acid. The effects of the laser fluence on the ablated particle size and concentration were investigated.

Experimental Section

A schematic diagram of the experimental apparatus is shown in Figure 1. Particles were produced by laser ablation of a thin matrix film on a stainless steel sample target. The sample target was held at the center of a 2.75 in. conflat tee and the laser entered the chamber through a quartz window. The volume of the chamber was 140 cm^3. The sample target was irradiated at normal incidence with a 337-nm nitrogen laser (VSL-337ND-S, LSI, Franklin, MA) operating at a repetition rate of 2 Hz. A 254-mm lens was used to focus the laser to a spot size of 250 $\times$ 250 μm^2. The spot size was measured by irradiating a small piece of laser burn paper (Pacific Coast Photo, Santa Cruz,CA) attached to the target and inspecting the burn mark visually with a measuring microscope. The laser energy was measured with a pyroelectric detector (ED-104AX, Gentec, Palo Alto, CA).

The particle ablation chamber was placed directly above an aerodynamic particle sizer (Model 3321, TSI, Shoreview, MN), which was used to determine the size distribution and concentration of the ablated aerosol particles. The particle sizer measures the velocity of particles in an accelerating air-flow through a nozzle. The flow rate into the instrument was 5 L/min for the results reported below. After entering the instrument, particles are confined to the centerline of the accelerating flow by sheath air, after which they pass through two focused 675 nm diode laser beams. The time difference between the two scattered-light pulses is used to determine the velocity of each particle that passes through the beams. The particle aerodynamic diameter is obtained from the velocity. Particles between 500 nm and 20 μm in aerodynamic size can be measured to a precision of 30 nm. Particle detection efficiency drops significantly for particles below 500 nm diameter; particles with diameters less than this size are recorded in a single channel due to the larger uncertainty in the size measurement in this range. For the data reported below, data from particles with aerodynamic diameters below 500 nm were not considered. Particle size measurements were initiated immediately after the target was irradiated with the laser and signal was integrated for a total of 5 s (10 laser shots).

Solid matrix samples were prepared by depositing 10 μL of the matrix solution on the sample target and allowing it to dry. The matrix solutions were 2,5-dihydroxybenzoic acid (DHB, Sigma, St. Louis, MO), 4-nitroaniline (Fluka, Ronkonkoma, NY), and sinapic acid (Fluka, Ronkonkoma, NY) at 20 mg/mL in methanol (Fisher, Fair Lawn, NJ) and 2-(4-hydroxyphenylazo)benzoic acid (HABA, Aldrich, Milwaukee, WI) at 20 mg/mL in a 70:30 (v/v) mixture of acetonitrile (Fisher, Fair Lawn, NJ) and 0.1% aqueous trifluoroacetic acid (Fisher, Fair Lawn, NJ). The resulting sample spots were approximately 7 mm in diameter.

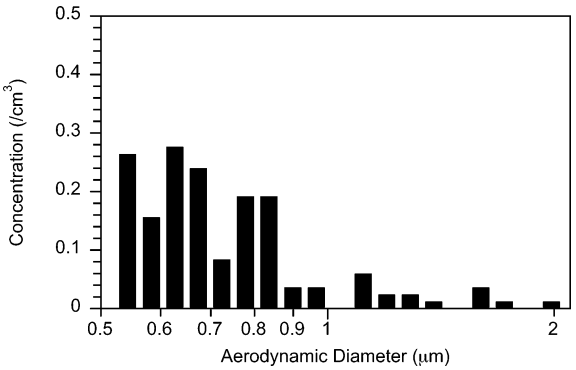

Figure 2. Coarse particle size distribution measured after irradiation of the stainless steel target at 500 J/m^2.

Results

The particle size distribution plot in Figure 2 gives an indication of the coarse particulate produced by irradiation of a nominally clean stainless steel target. The height of the vertical bar indicates the particle concentration measured in the indicated aerodynamic diameter range. At 500 J/m^2 fluence, the mean coarse particle diameter is 830 $\pm$ 30 nm and the total coarse particle concentration is 4.3 $\pm$ 0.2 per cm^3. Note that this mean diameter does not take into account particles below 500 nm that are not efficiently detected by the instrument. The error reported here and below was determined from one standard deviation resulting from five replicate runs. A total coarse particle concentration less than 5 per cm^3 was observed for blank target irradiation at all laser fluences.

Particle size distribution plots for the solid matrixes DHB, sinapic acid, 4-nitroaniline, and HABA are shown in Figure 3. The laser fluence was 500 J/m^2 in all cases. The mean size measured for the detected particles was approximately 700 nm at this fluence: 680 $\pm$ 20 nm for DHB, 710 $\pm$ 20 nm for sinapic acid, 670 $\pm$ 20 nm for 4-nitroaniline, and 710 $\pm$ 30 nm for HABA. With the exception of DHB, the smallest detected particles are the most abundant, suggesting that the peak of the size distribution may be below 500 nm. The ablated coarse particle concentration was lowest for sinapic acid and highest for HABA, but all were within 35% of 170 per cm^3 at this fluence. The measured values were 170 $\pm$ 20 per cm^3 for DHB, 120 $\pm$ 30 per cm^3 for sinapic acid, 150 $\pm$ 30 per cm^3 for 4-nitroaniline, and 230 $\pm$ 50 per cm^3 for HABA.

The effect of laser fluence on the coarse particle size distribution is shown in Figure 4. Ablated particle size distributions for DHB matrix were measured at 300, 500, 750, and 1100 J/m^2 and the data are plotted on a log scale so that the trends for low particle concentrations are readily observable. There is a noticeable shift from larger to smaller particle size with increasing laser fluence, which can be seen in Figure 5a and in Table 1. The measured mean coarse particle diameter decreases from 730 nm at 300 J/m^2 to 680 nm at 500 J/m^2, after which it remains constant to within the measured error. Associated with the decrease in coarse particle diameter is a linear increase in particle concentration, seen in Figure 5b and also in Table 1.

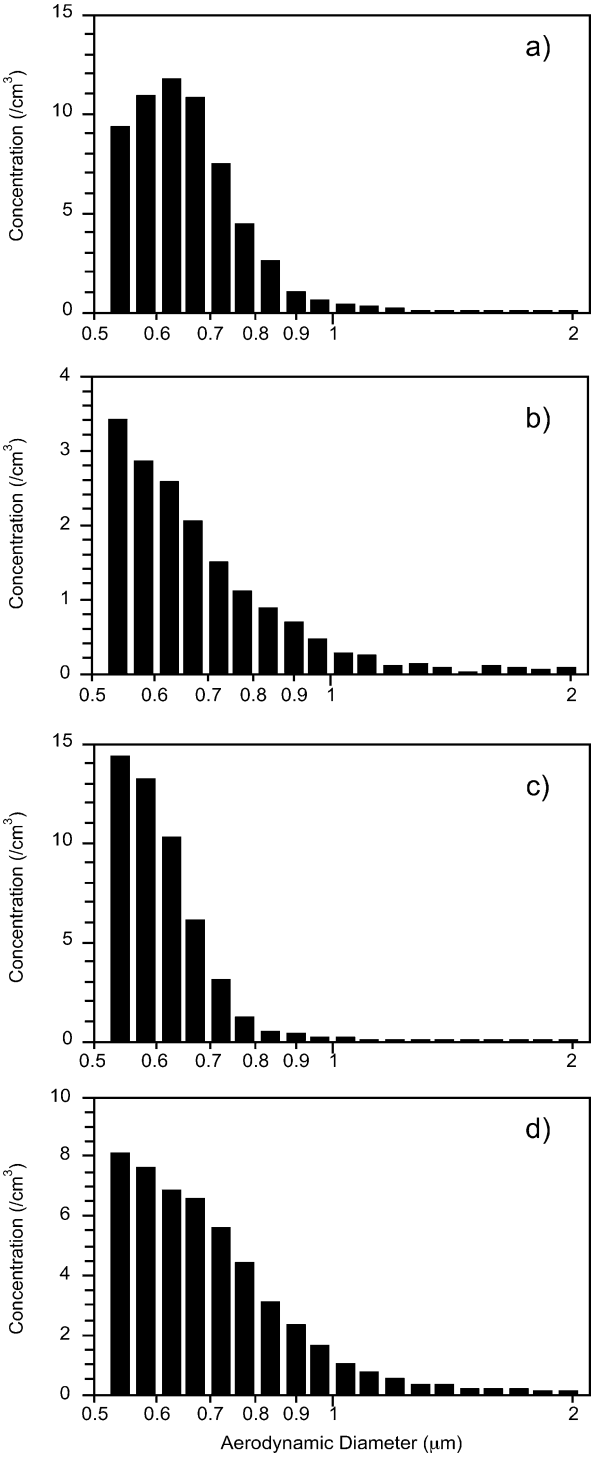

Figure 3. Coarse particle size distribution measured after 500 J/m^2 irradiation of thin films of (a) 2,5-dihydroxybenzoic acid, (b) sinapic acid, (c) 4-nitroaniline, and (d) 2-(4-hydroxyphenylazo)benzoic acid.

Particles are first observed above the background of 5 per cm^3 for laser fluence of 300 J/m^2, after which the concentration increases linearly to 800 per cm^3 at 1100 J/m^2.

Discussion

One of the most important issues in ablation of material in MALDI is the fraction of material that is removed as particulate. The quantity of material ejected per laser shot as micrometer sized particles can be estimated from the volume flow into the sizing instrument and the measured particle concentration. For example, DHB ablated at 2 laser shots per second at a thresohold

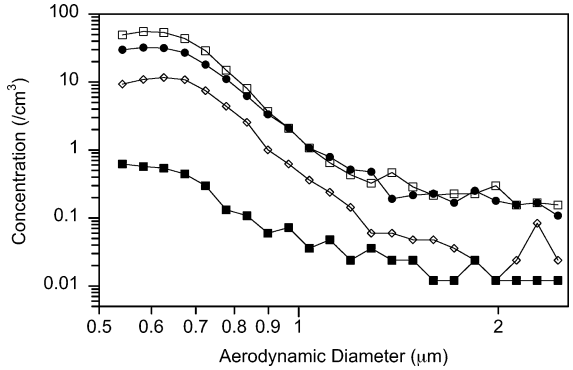

Figure 4. Distribution of coarse particle sizes resulting from ablation of a 2,5-dihydroxybenzoic acid thin film at 300 (squares), 500 (diamonds), 750 (circles), and 1100 J/m^2 (open squares).

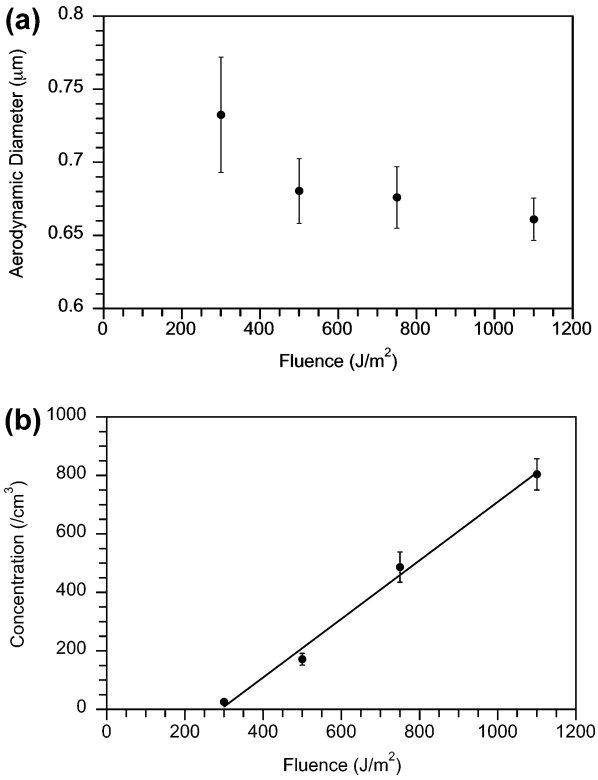

Figure 5. The fluence dependence of (a) coarse particle size and (b) coarse particle concentration for ablation of a 2,5-dihydroxybenzoic acid thin film.

TABLE 1: Size and Concentration Values for Coarse Particles Obtained at Different Laser Fluences for the DHB Matrix[a]

fluence (J/m^2)	mean coarse particle size (nm)	concn (per cm^3)
300	730(40)	30(5)
500	680(20)	170(20)
750	680(20)	490(50)
1100	660(15)	800(60)

[a] The measurement error represents one standard deviation obtained from five separate measurements. The reported mean coarse particle size includes only those particles larger than 500 nm that are efficiently detected by light scattering.

fluence of 300 J/m^2 produces a coarse particle concentration of 30 per cm^3. Combined with the flow rate of 80 cm^3/s, this corresponds to approximately 1000 particles per laser shot at threshold. The average diameter of these particles is 730 nm, resulting in an ejected volume of 200 μm^3 per laser shot. Using

a density for DHB of 1.4 g/cm^3, this ablated volume corresponds to approximately 2 pmol of DHB ejected per shot. Note that this estimated ejected volume does not include matrix monomers, clusters, or particulate below 500 nm in diameter.

The quantity of ablated matrix measured as micrometer-sized particulate can be compared to previous measurements of MALDI ablation volume. Several estimates have been made that are based on SEM measurements of ablation depth. Ablation of a DHB single crystal at 337 nm with 3000 J/m^2 fluence resulted in the removal of approximately of 100 μm^3 matrix per laser shot,[29] similar to the *particulate* volume estimated above. A similar study with a 355 nm UV laser at 600 J/m^2 fluence was used to estimate that 100 fmol of matrix was ablated per shot.[30] A recent study on quantifying MALDI sample consumption with use of ^{14}C-labeled analyte gave the result of 250 fmol of matrix removed per laser shot, using a 337 nm nitrogen laser.[31] The laser fluence was not reported in this study. Taken together, these studies indicate that between 100 fmol and 1 pmol of matrix is removed per laser shot in a typical MALDI analysis. Because we observe that several picomoles are ablated as micrometer-sized particulate, we conclude that under conditions similar to those used for MALDI, a significant fraction of the material removed is in the form of micrometer-sized particles.

The fluence threshold observed for coarse particle ablation is comparable to threshold values previously reported for analyte ion formation by MALDI. There is a wide variation in threshold fluences reported for MALDI, in part due to the difficulties in measuring the laser spot size. The typical method for spot size measurement is to observe the size of an ablated spot on the target generated by one or more laser shots. Since the size of the ablated spot depends on the material ablated, this measurement is subject to error. An additional consideration is the variation in laser energy across the beam. Unless special care is taken to produce a "flat-top" laser profile,[32] the fluence will not be constant across the laser beam. Threshold fluences as low as 10 J/m^2 and as high as 1000 J/m^2 have been reported; however, a typical value is in the range of 100 J/m^2.[10] The threshold for the formation of micrometer-sized particles from DHB matrix is 300 J/m^2 (Figure 5b), suggesting that the onset of particle formation is coincident or nearly coincident with the onset of ion formation. It is interesting to note that the fluence threshold for particle generation is similar to that observed for the ejection of material from a MALDI matrix and detected with a quartz microbalance.[33] In the microbalance study, two fluence thresholds were found. The first, at 100 J/m^2, was attributed to surface desorption of matrix monomers, and a second threshold at 300 J/m^2 was attributed to volume ejection. It is possible that this volume ejection process gives rise to the particulate ejection threshold detected in Figure 5b.

The decrease in size of coarse particles with increasing fluence that is observed in Figure 5a and the threshold fluence for particle formation are qualitatively consistent with recent molecular dynamics results.[8,9,34] The MD simulations show a sharp transition from molecular desorption to an explosive phase transition and ablation at fluences near the MALDI ion formation threshold. At fluences above threshold, the size of the ejected particulate drops due to the more vigorous phase explosion. A decrease in particle size with increasing fluence has been observed previously in the 266 nm ablation of glass to form micrometer-sized particles.[22] In trapping plate studies, the size of submicrometer particles formed in a vacuum by 337-nm ablation of DHB was found to decrease with increasing fluence.[28] A thin film resulting from molecular desorption was observed to increase in thickness with increasing fluence. These results were taken as an indication of an increase in molecular desorption with respect to particle ablation at higher fluences. Micrometer-sized particulate was not observed in these experiments, either because larger particles were not formed under vacuum or possibly due to a lower sticking coefficient for the larger particles.[33]

Conclusions

The number and size of micrometer-sized particles from 337 nm laser ablation of MALDI matrixes has been measured with a light-scattering particle-sizing instrument. The instrument is capable of detecting and counting particles between 500 nm and 20 μm in diameter. The mean coarse particle size (ignoring particles below 500 nm) for particles ablated from the matrixes 2,5-dihydroxybenzoic acid, sinapic acid, 4-nitroaniline, and 2-(4-hydroxyphenylazo)benzoic acid is approximately 700 nm. The fluence threshold was measured for 2,5-dihydroxybenzoic matrix and was found to be 300 J/m^2. This threshold is similar to the threshold for analyte ion formation in MALDI. The quantity of material ejected as micrometer-sized particulate is approximately 2 pmol, which is similar to the *total* quantity of material removed in a typical MALDI analysis. Taken together, these results suggest a possible correlation between particulate ablation and MALDI ion formation as has been suggested in several recent experimental and theoretical studies.[5−9]

Acknowledgment. This work was supported by National Science Foundation grant CHE-00196568, National Institutes of Health Grant R01ES10497, and Louisiana State University.

References and Notes

(1) Zenobi, R.; Knochenmuss, R. *Mass Spectrom. Rev.* **1999**, *17*, 337.
(2) Knochenmuss, R.; Stortelder, A.; Breuker, K.; Zenobi, R. *J. Mass Spectrom.* **2000**, *35*, 1237.
(3) Knochenmuss, R.; Zenobi, R. *Chem. Rev.* **2003**, *103*, 441.
(4) Breuker, K.; Knochenmuss, R.; Zhang, J.; Stortelder, A.; Zenobi, R. *Int. J. Mass Spectrom.* **2003**, *226*, 211.
(5) Karas, M.; Glückmann, M.; Schafer, J. *J. Mass Spectrom.* **2000**, *35*, 1.
(6) Karas, M.; Krüger, R. *Chem. Rev.* **2003**, *103*, 427.
(7) Karas, M.; Bahr, U.; Fournier, I.; Glückmann, M.; Pfenninger, A. *Int. J. Mass Spectrom.* **2003**, *226*, 239.
(8) Zhigilei, L. V.; Leveugle, E.; Garrison, B. J.; Yingling, Y. G.; Zeifman, M. I. *Chem. Rev.* **2003**, *103*, 321.
(9) Zhigilei, L. V.; Yingling, Y. G.; Itina, T. E.; Schoolcraft, T. A.; Garrison, B. J. *Int. J. Mass Spectrom.* **2003**, *226*, 84.
(10) Dreisewerd, K. *Chem. Rev.* **2003**, *103*, 395.
(11) Ehring, H.; Karas, M.; Hillenkamp, F. *Org. Mass Spectrom*. **1992**, *27*, 472.
(12) Zhigilei, L. V.; Kodali, P. B. S.; Garrison, B. J. *J. Phys. Chem. B* **1998**, *102*, 2845.
(13) Krüger, R.; Pfenninger, A.; Fournier, I.; Glückmann, M.; Karas, M. *Anal. Chem.* **2001**, *73*, 5812.
(14) Livadaris, V.; Blais, J.-C.; Tabet, J.-C. *Eur. J. Mass Spectrom.* **2000**, *6*, 409.
(15) Fournier, I.; Tabet, J. C.; Bolbach, G. *Int. J. Mass Spectrom.* **2002**, *219*, 515.
(16) Hankin, S. M.; John, P. *J. Phys. Chem. B* **1999**, *103*, 4566.
(17) Yeung, E. S.; Heise, T. W. *Anal. Chem.* **1992**, *64*, 2175.
(18) Puretzky, A. A.; Geohegan, D. B. *Chem. Phys. Lett.* **1998**, *286*, 425.
(19) Puretzky, A. A.; Geohegan, D. B.; Hurst, G. B.; Buchanan, M. V.; Luk'yanchuk, B. S. *Phys. Rev. Lett.* **1999**, *83*, 444.
(20) Puretzky, A. A.; Geohegan, D. B. *Appl. Surf. Sci.* **1998**, *127*−*129*, 248.
(21) Kimbrell, S. M.; Yeung, E. S. *Appl. Spectrosc.* **1991**, *45*, 442.
(22) Jeong, S. H.; Borisov, O. V.; Yoo, J. H.; Mao, X. L.; Russo, R. E. *Anal. Chem.* **1999**, *71*, 5123.
(23) Yoo, J. H.; Borisov, O. V.; Mao, X.; Russo, R. E. *Anal. Chem.* **2001**, *73*, 2288.
(24) Georgiou, S.; Koubenakis, A. *Chem. Rev.* **2003**, *103*, 349.

(25) Seto, T.; Kawakami, Y.; Suzuki, N.; Hirasawa, M.; Aya, N. *Nano Lett.* **2001**, *1*, 315.

(26) Ullmann, M.; Friedlander, S. K.; Schmidt-Ott, A. *J. Nanoparticle Res.* **2002**, *4*, 499.

(27) Mafune, F.; Kohno, J.; Takeda, Y.; Kondow, T. *J. Phys. Chem. B* **2003**, *107*, 4218.

(28) Handschuh, M.; Nettesheim, S.; Zenobi, R. *Appl. Surf. Sci.* **1999**, *137*, 125.

(29) Strupat, K.; Karas, M.; Hillenkamp, F. *Int. J. Mass Spectrom. Ion Proc.* **1991**, *111*, 89.

(30) Westman, A.; Huth-Fehre, T.; Demirev, P.; Sundqvist, B. U. R. *J. Mass Spectrom.* **1995**, *30*, 206.

(31) Page, J. S.; Sweedler, J. V. *Anal. Chem* **2002**, *74*, 6200.

(32) Dreisewerd, K.; Schuerenberg, M.; Karas, M.; Hillenkamp, F. *Int. J. Mass Spectrom. Ion Proc.* **1995**, *141*, 127.

(33) Quist, A. P.; Huth-Fehre, T.; Sundqvist, B. U. R. *Rapid Commun. Mass Spectrom.* **1994**, *8*, 149.

(34) Itina, T. E.; Zhigilei, L. V.; Garrison, B. J. *J. Phys. Chem. B* **2002**, *106*, 303.